

RESEARCH ARTICLE

Planar cell polarity signaling regulates polarized second heart field morphogenesis to promote both arterial and venous pole septation

Ding Li, Allyson Angermeier and Jianbo Wang*

ABSTRACT

The second heart field (SHF) harbors progenitors that are important for heart formation, but little is known about its morphogenesis. We show that SHF population in the mouse splanchnic mesoderm (SpM-SHF) undergoes polarized morphogenesis to preferentially elongate anteroposteriorly. Loss of *Wnt5a*, a putative ligand of the planar cell polarity (PCP) pathway, causes the SpM-SHF to expand isotropically. Temporal tracking reveals that the *Wnt5a* lineage is a unique subpopulation specified as early as E7.5, and undergoes bi-directional deployment to form specifically the pulmonary trunk and the dorsal mesenchymal protrusion (DMP). In *Wnt5a*^{-/-} mutants, *Wnt5a* lineage fails to extend into the arterial and venous poles, leading to both outflow tract and atrial septation defects that can be rescued by an activated form of PCP effector Daam1. We identify oriented actomyosin cables in the medial SpM-SHF as a potential *Wnt5a*-mediated mechanism that promotes SpM-SHF lengthening and restricts its widening. Finally, the *Wnt5a* lineage also contributes to the pulmonary mesenchyme, suggesting that *Wnt5a*/PCP is a molecular circuit recruited by the recently identified cardiopulmonary progenitors to coordinate morphogenesis of the pulmonary airways and the cardiac septations necessary for pulmonary circulation.

This article has an associated 'The people behind the papers' interview.

KEY WORDS: Morphogenesis, Planar cell polarity, Second heart field

INTRODUCTION

Formation of the heart requires precise coordination of fate specification, proliferation, differentiation and morphogenesis (Evans et al., 2010). In the mouse and chick, cardiogenic progenitors that will give rise to the four-chambered heart are initially specified in the anterior lateral plate mesoderm during gastrulation. Subsequent embryo folding brings the cardiogenic progenitors in the two lateral regions to the ventral midline, where they fuse to form the initial heart tube known as the first heart field (FHF). At the same time, the cardiogenic progenitors in the medial region are displaced dorsally to form the second heart field (SHF). FHF cells undergo myocardial differentiation to become the left ventricle and part of the atria, whereas SHF cells remain undifferentiated and proliferate as multipotent progenitors. Progressive differentiation and deployment of SHF cells elongate the early heart tube to promote cardiac looping and to build additional parts of the heart, including the right ventricle, outflow tract

(OFT), atria and atrial septum. Abnormal development of the SHF contributes frequently to a spectrum of congenital heart defects (CHDs), including atrioventricular septal defects (AVSDs) and conotruncal defects such as common arterial trunk (CAT) and double outlet right ventricle (DORV) (Bruneau, 2008; Kelly, 2012). Thorough understanding of SHF development will provide key insight into diagnosis, prevention and therapies of CHDs.


The SHF can be broadly divided into two regions: the pharyngeal/branchial arch region residing rostral and dorsal to the OFT and contributing solely to the arterial pole of the heart, and the splanchnic mesoderm (SpM-SHF) region that lies caudal to the OFT and contributes to both the arterial and venous poles. Studies in the field have elucidated how rostral-caudal patterning and proliferation/differentiation in the SHF can be regulated by interplay between multiple signaling pathways and complex epigenetic and transcriptional networks (Chang and Bruneau, 2012; Evans et al., 2010; McCulley and Black, 2012). By contrast, the morphogenetic aspect of SHF development remains largely unknown. For example, cells proliferate rapidly in the caudal SpM-SHF of avian embryos (van den Berg et al., 2009), but how the SpM-SHF grows and expands at the tissue level was not known. In some tissues, such as the limb bud mesenchyme, rapid proliferation does not lead to isotropic expansion, but is associated with proximal-distal (P-D) extension that is vital for forming distal limb skeletal elements (Boehm et al., 2010; Gros et al., 2010).

In this study, we have investigated tissue level morphogenesis in the SHF, and how it can be affected by the planar cell polarity (PCP) signaling pathway. PCP was initially discovered in *Drosophila* and refers to cellular polarity in the plane of the epithelium, perpendicular to the apicobasal polarity. As a branch of the non-canonical Wnt signaling pathway, the PCP pathway shares Frizzled (Fz) receptor and cytoplasmic protein Dishevelled (Dvl/Dsh) with the canonical Wnt pathway, but does not result in β -catenin stabilization. Instead, Fz and Dvl/Dsh interact with a set of core PCP proteins, such as Van gogh (Vang), to coordinate cell polarity (Bayly and Axelrod, 2011; Goodrich and Strutt, 2011; Humphries and Mlodzik, 2018). In vertebrates, core PCP proteins have also been shown to regulate convergent extension (CE), a morphogenesis process where directional cell behaviors promote simultaneous tissue elongation and narrowing (Goodrich and Strutt, 2011; Huebner and Wallingford, 2018). Work in *Xenopus* and zebrafish has identified that non-canonical Wnt ligands, e.g. *Wnt5a* and *Wnt11*, act upstream of core PCP proteins to modulate cytoskeleton dynamics, cell adhesion and protrusion activity, etc. during CE. These cellular events are mediated by a range of downstream effectors, including small GTPases Rho/Rac/Cdc42/Rab5, JNK and Daam1 (Dishevelled associated activator of morphogenesis 1) in a cell type- and tissue-specific manner (Butler and Wallingford, 2017; Devenport, 2016).

In mice, germline deletion of *Wnt5a*, which encodes a presumptive mammalian PCP ligand, leads to CAT with almost full penetrance, whereas disruption of other PCP genes, *Wnt11*,

Department of Cell, Developmental and Integrative Biology, School of Medicine, University of Alabama at Birmingham, Birmingham, AL 35226, USA.

*Author for correspondence (j18wang@uab.edu)

 J.W., 0000-0002-6769-9851

Received 18 June 2019; Accepted 23 August 2019

Dvl1/2/3 and *Vangl2* (*Vang like 2*), causes a spectrum of OFT defects from DORV to CAT (Etheridge et al., 2008; Person et al., 2010; Ramsbottom et al., 2014; Sinha et al., 2012; van Vliet et al., 2017). Although the defects in these mutants have all been attributed to OFT shortening, the cause of which varies. Analysis of *Wnt11* and *Vangl2* revealed that they are required within OFT myocardium for cell polarization and organization during OFT elongation (Ramsbottom et al., 2014; van Vliet et al., 2017). In contrast, we and others have found that *Wnt5a* is highly expressed in the caudal SpM-SHF but not the OFT (Chen et al., 2012; Li et al., 2016; Sinha et al., 2015a, 2012). The expression pattern and the aberrant cell polarity, morphology and packing in the caudal SpM-SHF of *Wnt5a* and *Dvl1/2* mutants led us to postulate that a *Wnt5a*→*Dvl* PCP signaling cascade promotes deployment of SpM-SHF cells to the OFT for its elongation, likely by inducing polarized cell intercalation to incorporate mesenchymal-like SHF progenitors into a cohesive epithelial-like sheet (Sinha et al., 2012). Other studies have confirmed that the ventral-most layer of the SpM-SHF, which forms the dorsal wall of the pericardial cavity, indeed gains epithelial property and becomes contiguous with the inferior OFT myocardium (Francou et al., 2017, 2014; Ramsbottom et al., 2014). In support of our model, *Wnt5a* null mutants display diminished inferior OFT myocardium and its derivative subpulmonary myocardium (Sinha et al., 2015a).

These findings prompted us to ask the broader question of how SHF morphogenesis occurs and what role *Wnt5a*/PCP may play. We show that *Wnt5a* promotes SpM-SHF lengthening while restricting its widening and thickening, and identify the *Wnt5a* lineage as a unique subset of SpM-SHF population that undergoes bi-directional deployment to form specifically the pulmonary trunk and the DMP (dorsal mesenchymal protrusion). *Wnt5a* lineage in

the SpM-SHF also contributes extensively to the pulmonary mesenchyme. Given the recent finding that the caudal SpM-SHF harbors cardiopulmonary progenitors that coordinate heart and lung development (Peng et al., 2013; Steimle et al., 2018), our findings suggest the intriguing idea that *Wnt5a*/PCP-mediated SpM-SHF morphogenesis may orchestrate two processes: (1) promoting deployment of SHF cells to the heart to separate pulmonary from systemic circulation; and (2) driving A-P elongation for proper morphogenesis of the respiratory airway.

RESULTS

Loss of *Wnt5a* disrupts polarized morphogenesis of the SpM-SHF

To analyze morphogenesis of the SpM-SHF, we first performed genetic labeling using *Mef2c-Cre* (Verzi et al., 2005) together with Cre reporter *Rosa26^{td-Tomato}* (Madisen et al., 2010). We stained serial sagittal sections of *Mef2c-Cre*; *Rosa26^{td-Tomato}* embryos harvested from E8.5 to E11.5 with the myocardial marker cTnT (cardiac troponin T), and defined SpM-SHF as the contiguous population of undifferentiated myocardial progenitors that were labelled by td-Tomato but negative for cTnT staining, and located caudal and dorsal to the OFT (Fig. S1).

Three-dimensional (3D) reconstruction of serially sectioned wild-type embryos revealed that, from E9.0 to E10.0, the SpM-SHF extends rostrally, resulting in a small triangular protrusion behind the OFT and the aortic sac (red arrows, Fig. 1B,J). This protrusion is likely to form part of the aortopulmonary septal complex in the back wall of the aortic sac, which will fuse with the distal OFT cushions to divide the OFT into aortic and pulmonary channels (Anderson et al., 2012). Subsequently from E10.0 to E11.5, as the SpM-SHF elongates further along the anteroposterior (AP)

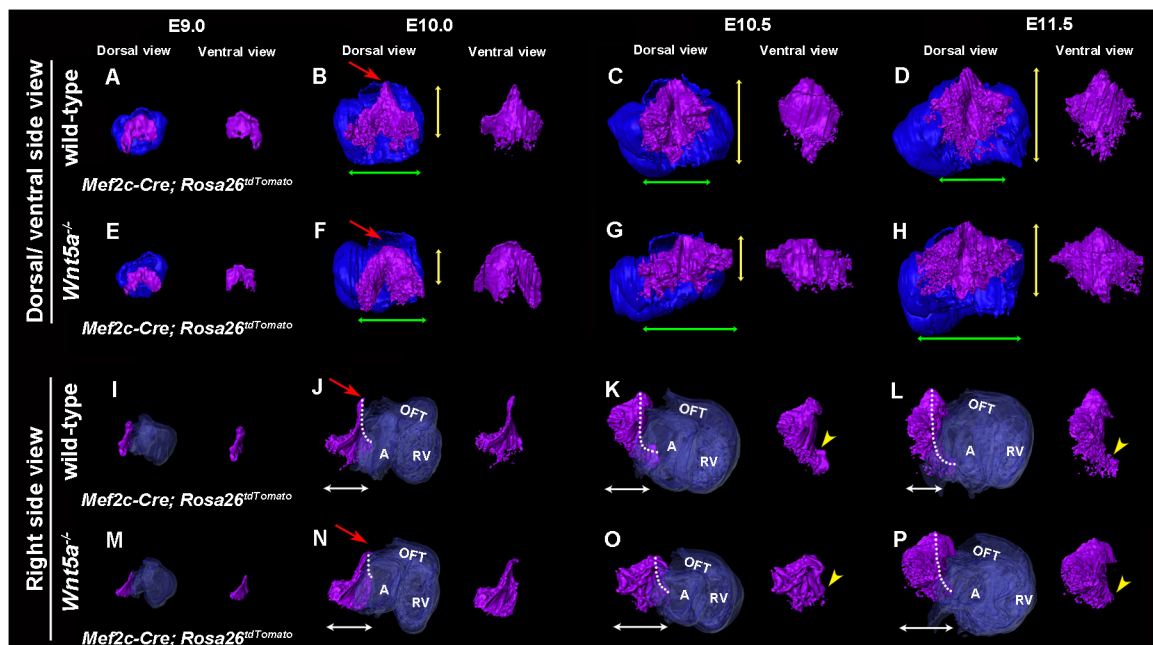


Fig. 1. Loss of *Wnt5a* disrupts polarized morphogenesis of the SpM-SHF. (A–P) The SpM-SHF was labeled using *Mef2c-Cre* and *Rosa26^{td-Tomato}* reporter (purple). The myocardium is shown in blue. Dorsal/ventral and side views of 3D reconstructed images show that in wild type, the SpM-SHF extends rostrally from E9.0 to E10.0, forming a triangular structure behind the dorsal wall of the aortic sac/OFT (red arrows, B,J). The SpM-SHF elongates further from E10.0 to E11.5 (yellow double-headed arrows, B–D; dotted lines, J–L), but does not significantly widen (green double-headed arrows, B–D) or thicken (white double-headed arrows, J–L). In wild type, the SpM-SHF also extended caudally into the atria to form the DMP (yellow arrowheads, K,O). In *Wnt5a*^{−/−} mutants, the SpM-SHF elongates less efficiently (yellow double-headed arrows, F–H, white dotted lines, N–P), and fails to extend either rostrally to the OFT at E10.0 (red arrows, F,N) or caudally into the atria by E10.5 (yellow arrowhead, O). Instead, the SpM-SHF becomes significantly widened (F–H) and thickened (N–P). A less prominent DMP forms in the mutants by E11.5 (yellow arrowhead, P).

axis (dotted lines, Fig. 1J-L), it also starts to protrude caudally into the atria (yellow arrowheads, Fig. 1K,O). This is consistent with the reports that *Mef2c-Cre* labeled SpM-SHF lineage gives rise to the DMP that forms part of the atrial septal complex (Briggs et al., 2013; Goddeeris et al., 2008; Xie et al., 2012).

Importantly, our morphometric analyses reveal that SpM-SHF morphogenesis occurs in a highly polarized fashion. As the overall size of the SpM-SHF enlarges from E10.0 to 11.5, its length appears to increase more significantly than its width and thickness (Fig. 1B-D: yellow double-headed arrows, length; green double-headed arrows, width; Fig. 1B-D; Fig. 1J-L: white double-headed arrow, thickness). To assess these changes quantitatively, we calculated the length-to-width ratio (LWR) and the length-to-thickness ratio (LTR) at each stage. We found that from E10.0 to 11.5, the LTR increases by 22%, and the LWR increases twofold (Table 1). Our data therefore suggest that the SpM-SHF grows not by isotropic expansion, but through concomitant lengthening and narrowing, a phenomenon reminiscent of CE.

As CE is regulated by PCP signaling and a PCP ligand, *Wnt5a*, is specifically expressed in the caudal half of the SpM-SHF (Li et al., 2016; Sinha et al., 2015a), we studied SpM-SHF morphogenesis in *Wnt5a* null mice. At E8.5 and 9.0, the morphology of the SpM-SHF in *Wnt5a*^{-/-} mutant embryos is similar to that in wild types (Fig. 1A, E; Fig. S2). Shortly afterwards, however, the SpM-SHF in *Wnt5a*^{-/-} mutants starts to display reduced lengthening (Fig. 1F-H,N-P) and fails to extend rostrally to form the triangular protrusion behind OFT by E10.0 (red arrows, Fig. 1F,N). By E10.5, it also fails to extend caudally into the atria to form the DMP (Fig. 1O).

Concurrent with the lengthening defect, the SpM-SHF in *Wnt5a*^{-/-} mutants becomes widened (Fig. 1F-H) and thickened (Fig. 1N-P). As a result, the LWR of the SpM-SHF remains unchanged from E10.0 to 11.5 in *Wnt5a*^{-/-} mutants, in contrast to the twofold increase in wild type (Table 1). Furthermore, whereas the LTR of the SpM-SHF is increased by 22% in wild type, it is decreased by 21% in *Wnt5a*^{-/-} mutants. Despite the significant morphological change, the total volume of the SpM-SHF remains comparable between *Wnt5a* mutants and wild type at each stage, consistent with the fact that there is no cell proliferation or apoptosis defects in *Wnt5a* mutant SHF (Li et al., 2016; Sinha et al., 2012). These data indicate that loss of *Wnt5a* is sufficient to disrupt polarized, CE-like morphogenesis in the SpM-SHF.

Loss of *Wnt5a* in the SHF causes atrial septation defect

The DMP is important for atrial septation as it bridges the gap between the primary atrial septum (PAS) and the atrioventricular cushions (AVCs) (Briggs et al., 2012; Snarr et al., 2007a; Xie et al., 2012). The significant DMP shortening in E10-11.5 *Wnt5a* mutants suggested that they might display atrial septation defects. We

therefore performed 3D reconstruction on E13.5 embryos. We found that in wild-type embryos, the DMP has already extended to completely fill the gap between the PAS and AVCs (Fig. 2A-D', red arrow), but it fails to do so in *Wnt5a*^{-/-} mutants (Fig. 2E-H', white arrowhead). This leads to incomplete atrial septation and a form of AVSD known as primum atrial septal defect (ASD), which is confirmed on transverse sections (Fig. 2J, white arrowhead).

The primum ASD continues to be observed in *Wnt5a*^{-/-} mutants recovered at E16.5 and P0 (Fig. 2L and data not shown), indicating that it is not due to a developmental delay. Eight out of nine *Wnt5a*^{-/-} embryos examined between E13.5 and P0 displayed the defect, whereas no such defect was detected in nine *Wnt5a*^{+/+} or *Wnt5a*^{+/-} littermates. Associated with the ASD, *Wnt5a*^{-/-} mutants continues to display significant widening, thickening and shortening of the SpM-SHF (compare Fig. 2A with E and 2D with H). Collectively, these data (Figs 1 and 2) support the idea that, through regulating polarized SpM-SHF morphogenesis to promote DMP elongation, *Wnt5a* plays an important role for atrial septal formation. Furthermore, *Tbx1* has been shown to activate *Wnt5a* transcription in the caudal SpM-SHF (Chen et al., 2012), and loss of *Tbx1* also causes primum ASD (Rana et al., 2014). Therefore, *Tbx1* may activate *Wnt5a* expression for both arterial and venous pole development.

To further determine whether the ASD in *Wnt5a*^{-/-} null mutants is due specifically to loss of *Wnt5a* function within the SHF, we first removed *Wnt5a* in the SHF using a floxed *Wnt5a* allele (Ryu et al., 2013) and *Isl1-Cre* (Yang et al., 2006). We found that loss of *Wnt5a* in *Isl1-Cre* lineage is sufficient to recapitulate both the ASD and OFT defects observed in *Wnt5a*^{-/-} mutants (Fig. S2A-D). Conversely, we tested rescuing the ASD in *Wnt5a*^{-/-} mutants by restoring *Wnt5a* solely in the SHF using *Mef2c-Cre* and *Rosa26^{Wnt5a}*, a *Wnt5a* conditional gain-of-function allele (Cha et al., 2014; Li et al., 2016). As we described before (Li et al., 2016), broadly overexpressing *Wnt5a* in the SHF cause embryonic lethality at E12.5 for a yet unknown reason. When we examined the embryos at E11.5, however, we found that SHF-specific *Wnt5a* overexpression was sufficient to restore both DMP extension and SpM lengthening in *Wnt5a*^{-/-} mutants (Fig. S2F-G"). Together, these complementary loss- and gain-of-function studies indicate that *Wnt5a* is required specifically in the SHF for proper DMP formation.

Wnt5a lineage tracing reveals polarized and temporally distinct deployment pattern of SHF progenitors to form the pulmonary trunk and DMP

Our findings so far support the idea that *Wnt5a*-regulated morphogenesis of SpM-SHF cells promotes their deployment for both OFT and DMP formation. Both *Wnt5a* mRNA and protein, however, are expressed only in the caudal SpM (Li et al., 2016;

Table 1. Morphometric measurement of the SpM-SHF from E9.0 to E11.5

	Wild type			<i>Wnt5a</i> ^{-/-}		
	E10.0	E10.5	E11.5	E10.0	E10.5	E11.5
Volume (voxel ×10 ³)	352.7±43.1	876.8±46.7	1037.2±43.1	344.6±63.1 N.S.	883.2±69.1 N.S.	1038.7±130.0 N.S.
Average length (μm)	34.5±1.9	60.4±1.7	67.0±4.6	27.8±1.2*	37.9±6.5*	45.1±6.4*
Average width (μm)	39.6±2.4	38.9±2.7	38.6±4.3	38.1±1.5 N.S.	52.5±2.0*	58.4±2.7*
Average thickness (μm)	17.3±1.6	23.9±0.86	27.7±1.8	22.4±2.5*	43.9±0.2*	45.8±3.8*
Length-to-width ratio (LWR)	0.87	1.55	1.74	0.73	0.72	0.77
Length-to-thickness ratio (LTR)	1.99	2.53	2.42	1.24	0.86	0.98

Data are mean±s.e.m.

**P*<0.05 between *Wnt5a* mutant and wild-type embryos of the same stage; N.S, non-significant.

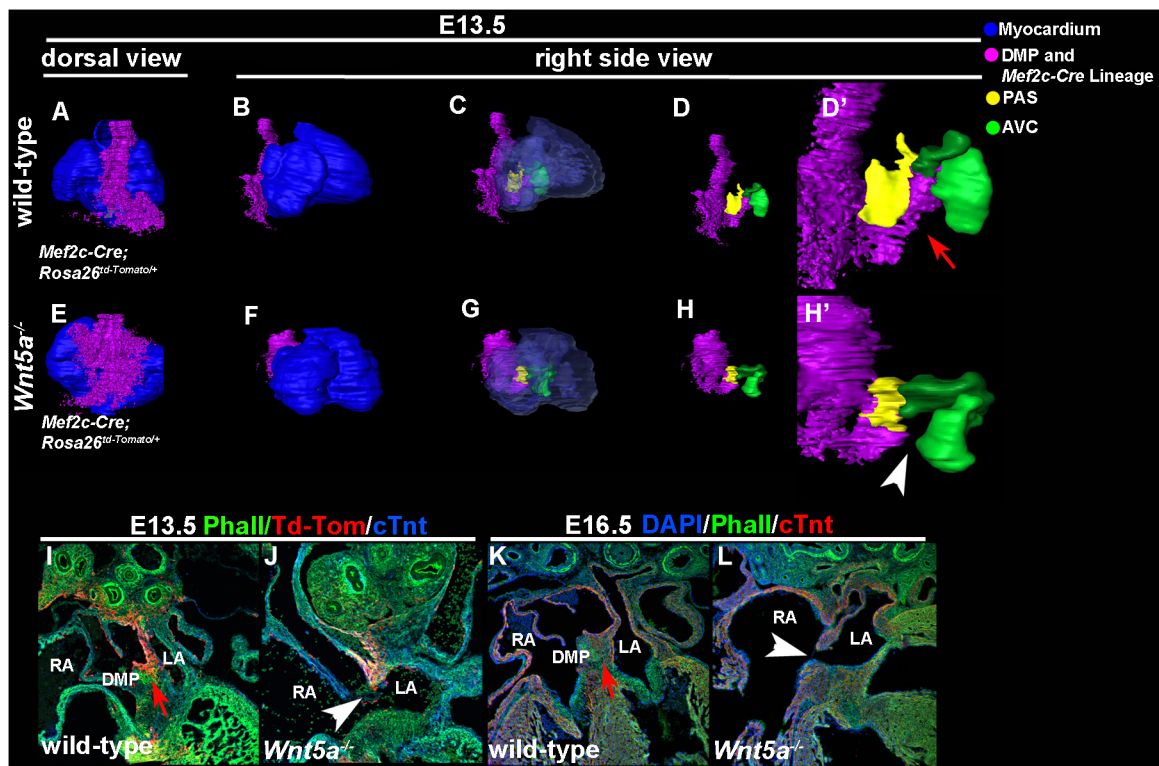


Fig. 2. Loss of *Wnt5a* causes atrial septation defect. (A-H') 3D reconstruction of E13.5 embryos showed that the SpM-SHF (purple) displays significantly widened, thickened and shortened morphology in *Wnt5a*^{-/-} mutants (compare A with E and D with H). In wild type, the SpM-SHF-derived DMP (red arrow, D') has already extended into the atria to completely fill the gap between the primary atrial septum (PAS, yellow) and the atrioventricular cushions (AVCs, green). In *Wnt5a*^{-/-} mutants, the DMP fails to extend sufficiently to fill the gap (white arrowhead, H'). (I-L) On transverse sections, a septum has already formed to completely septate the right and left atrium in wild type at E13.5 and E16.5 (red arrows, I,K). In *Wnt5a*^{-/-} mutants, DMP-derived atrial septum is missing (white arrowheads, J,L).

Sinha et al., 2015a, 2012; Yamaguchi et al., 1999). This expression pattern suggests two possibilities: (1) *Wnt5a* could be expressed transiently in all SpM-SHF progenitors prior to their deployment; or (2) *Wnt5a* could be expressed only in a specific subset of SpM-SHF progenitors. To gain insight into this issue, we labeled *Wnt5a*-expressing cells and tracked their morphogenesis and deployment pattern to the heart.

To label *Wnt5a* lineage genetically, we created a *Wnt5a*-CreER BAC (bacterial artificial chromosome) transgene by inserting tamoxifen-inducible CreER T2 into a 198 kb BAC clone containing the mouse *Wnt5a* locus. After crossing *Wnt5a*-CreER with *Rosa26*^{td-Tomato} Cre reporter mice, we administered tamoxifen at various embryonic stages. When tamoxifen was administered at or before E6.5, we could not detect any labeled cells in the SHF region at E9.5–11.5. But when we gave tamoxifen at E7.5 or E8.5 and examined the embryos at E8.75 or 9.75, respectively, we found that td-Tomato positive cells were located specifically at the caudal SpM-SHF, near the atria (see Fig. 4A–A" and data not shown). This pattern closely mimics the temporal and spatial expression of *Wnt5a* mRNA and protein (Fig. S3) (Li et al., 2016; Schleiffarth et al., 2007; Sinha et al., 2015a, 2012; Yamaguchi et al., 1999), indicating that the *Wnt5a*-CreER transgene is able to recapitulate *Wnt5a* expression in the SHF.

We then performed long-term lineage tracing to determine the contribution of *Wnt5a*-expressing cells to the heart. We performed single-dose tamoxifen treatment at E7.5, E8.5 or E9.5 (Fig. 3A–B"; C–D"; E–F"), or triple-dose tamoxifen treatments at E7.5, E8.5 and E9.5 (Fig. 3G–H"). When we analyzed the resulting embryos at E13.5, we found that td-Tomato-labeled cells at the venous pole (Fig. 3A,C, E,G) contributed primarily to the DMP. At the arterial pole (Fig. 3B,

D,F,H), they are located predominantly in the pulmonary trunk. These cells are mostly negative for cTnt (Fig. 3B",D",F",H") but positive for SMA (smooth muscle actin; Fig. 3H') staining, indicating that they are smooth muscle cells and not cardiomyocytes. Irrespective of the timing or dose of tamoxifen treatment, we observed similar labeling pattern in both the DMP and pulmonary trunk, although triple tamoxifen treatment resulted in more labeled cells (Fig. 3G–H"), whereas single tamoxifen treatment at E9.5 tend to give the fewest number of labeled cells (Fig. 3E–F"). When we administered tamoxifen at or after E10.5, we could no longer detect td-Tomato-labeled cells in either the pulmonary trunk or the DMP (data not shown). Therefore, *Wnt5a*-expressing cells between E7.5 and E9.5 represent a unique subpopulation of SHF progenitors fated to form predominantly the DMP and smooth muscle cells of the pulmonary trunk.

We found that *Wnt5a*-CreER-expressing cells labeled between E7.5–9.5 also contribute to structures outside of the heart. These mostly include the mesenchyme of the bronchi and trachea, smooth muscle cells of the lung airway and pulmonary arteries, myocardium of the pulmonary vein, and endothelium of the pulmonary arteries and vein (Fig. 3 and data not shown). These data indicate that *Wnt5a* lineage either overlaps with or is encompassed within the pSHF that has been shown to contain multipotent cardiopulmonary progenitors contributing to both the lung mesenchyme and venous pole of the heart (Peng et al., 2013; Steimle et al., 2018). Indeed, conditional deletion of *Wnt5a* using *Mef2c*Cre is sufficient to cause upper airway morphogenetic defects, including shortening and widening of the trachea (Fig. S6).

To further study morphogenesis and deployment of *Wnt5a* lineage to the heart and how these processes might be affected

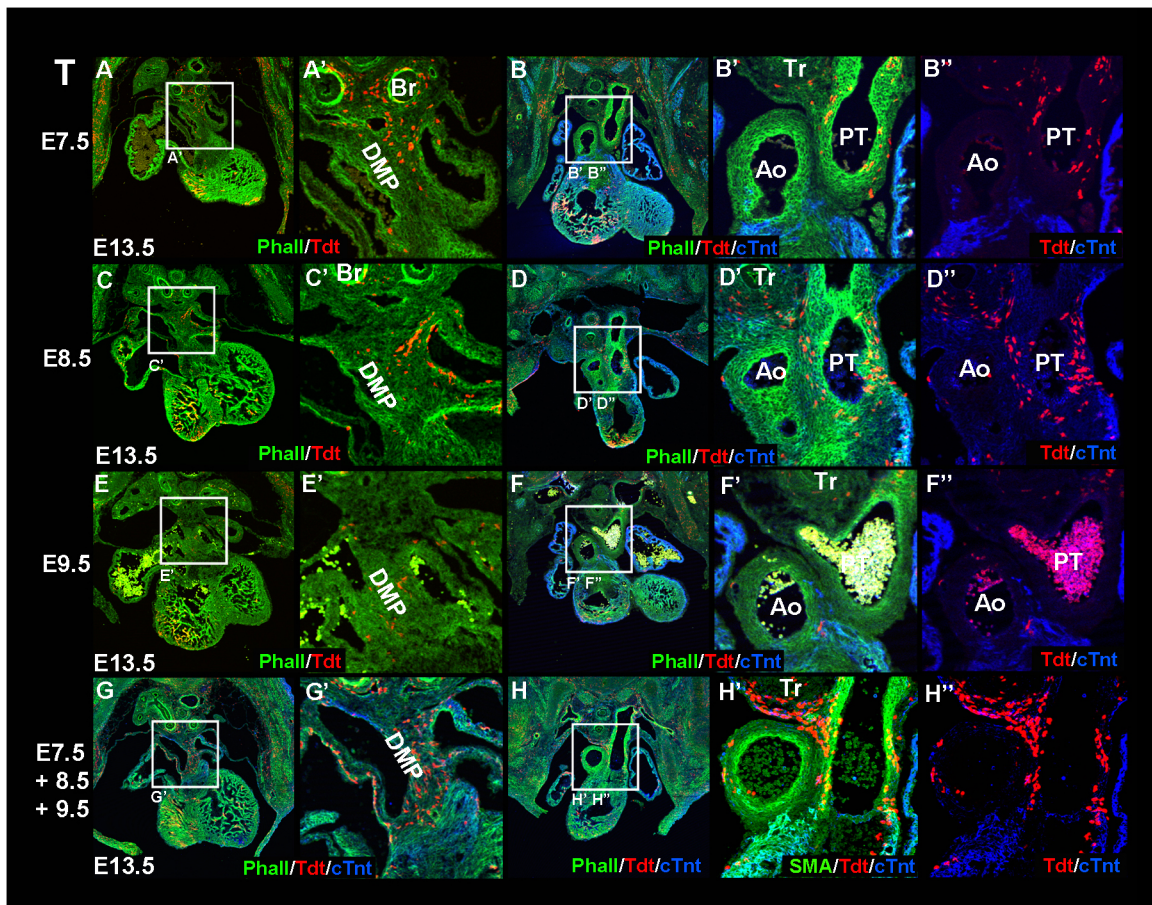


Fig. 3. The *Wnt5a* lineage contributes to both the arterial and venous poles of the heart. (A-H'') In *Wnt5a*CreER; *Rosa26*^{td-Tomato} embryos, Cre activity was induced by either a single dose (A-F'') or by three sequential daily doses of tamoxifen (T) from E7.5 to E9.5 (G-H''), and analyzed at E13.5. At the venous pole (A,A',C,C',E,E') of single-dose tamoxifen-induced embryos, td-Tomato (Tdt) labeled cells are observed in the DMP, whereas at the arterial pole (B-B'',D-D'',F-F'') almost all Tdt-labeled cells are situated in the non-myocardial (cTnt negative) tissues surrounding the pulmonary trunk. Triple dose-induced embryos display similar patterns but a larger number of Tdt-labeled cells in both DMP and pulmonary trunk (G-H''). Anti-SMA antibody staining indicates that the *Wnt5a* lineage in pulmonary trunk contains primarily smooth muscle cells (H'). *Wnt5a* lineage cells also contribute to the mesenchyme of the bronchi (Br) and trachea (Tr).

following loss of *Wnt5a*, we performed detailed temporal analyses. As activation of *Wnt5a*-CreER at any time between E7.5 and E9.5 labels similar components in the heart (Fig. 3), we administered a single dose of tamoxifen at E7.5 and examined embryos sequentially from E8.75 to E13.5. In wild type, we found that td-Tomato-labeled cells are initially located at the caudal SpM-SHF at E8.75 (Fig. 4A-A''). Their descendants first undergo an anteriorly oriented deployment towards the OFT at E9.5, enter the inferior OFT at E10.5 and E11.5 (Fig. 4C-C'',E-E'',G-G''), and form the pulmonary trunk by E13.5 (Fig. 4I-I''). From E11.5, some td-Tomato-labeled cells also started to extend posteriorly into the atria (Fig. 4G-G'') and to form the DMP to septate the atria by E13.5 (Fig. 4I-I''); Movie 1, color code as in Fig. 4). Therefore, *Wnt5a*-expressing cells appear to undergo two polarized, temporally distinct deployment processes: an arterial pole deployment that initiates between E9.0 and E9.5 to form the distal inferior OFT and ultimately the pulmonary trunk; and a venous pole deployment that starts between E10.5 and E11.5 to extend into the atria and form the DMP.

When we examined *Wnt5a*^{-/-} littermates, we found that td-Tomato-labeled cells are initially located properly at the caudal SpM-SHF at E8.75 (Fig. 4B-B''), indicating that the early specification and localization of the *Wnt5a* lineage are not disrupted in *Wnt5a*^{-/-} mutants. By E9.5, however, almost all td-Tomato-labeled cells

remain around the venous pole and very few of them are deployed anteriorly (Fig. 4D-D''); at E10.5 and E11.5, essentially no td-Tomato-labeled cells are able to enter the OFT (Fig. 4F-F'',H-H''). At E13.5, td-Tomato-labeled cells fail to contribute to any structure of the common arterial trunk (CAT) in *Wnt5a*^{-/-} mutants (Fig. 4J-J''; Movie 2). These results indicate that deployment of *Wnt5a* lineage anteriorly to the arterial pole is abolished in *Wnt5a*^{-/-} mutants. As the *Wnt5a* lineage normally gives rise to the smooth muscle lining of the pulmonary trunk (Fig. 3H'), their failure to deploy and contribute to the OFT could be a direct cause of CAT in *Wnt5a*^{-/-} mutants.

The posteriorly oriented deployment of *Wnt5a* lineage into the atria is also delayed in *Wnt5a*^{-/-} mutants and fails to occur at E11.5 (Fig. 4H''). By E13.5, however, some td-Tomato-labeled cells are able to extend into the atria to form a DMP, which appears shortened and fails to fill the gap between the PAS and AVCs. Together with our prior findings (Fig. 2), these data indicate that compromised posterior deployment of *Wnt5a*-expressing SHF cells is the cause of atrial septation defects in *Wnt5a* mutants.

***Wnt5a* regulates biased actomyosin distribution during SpM-SHF morphogenesis**

In our earlier studies, we proposed that *Wnt5a* may regulate polarized cell intercalation along the D-V axis (Sinha et al., 2015a,

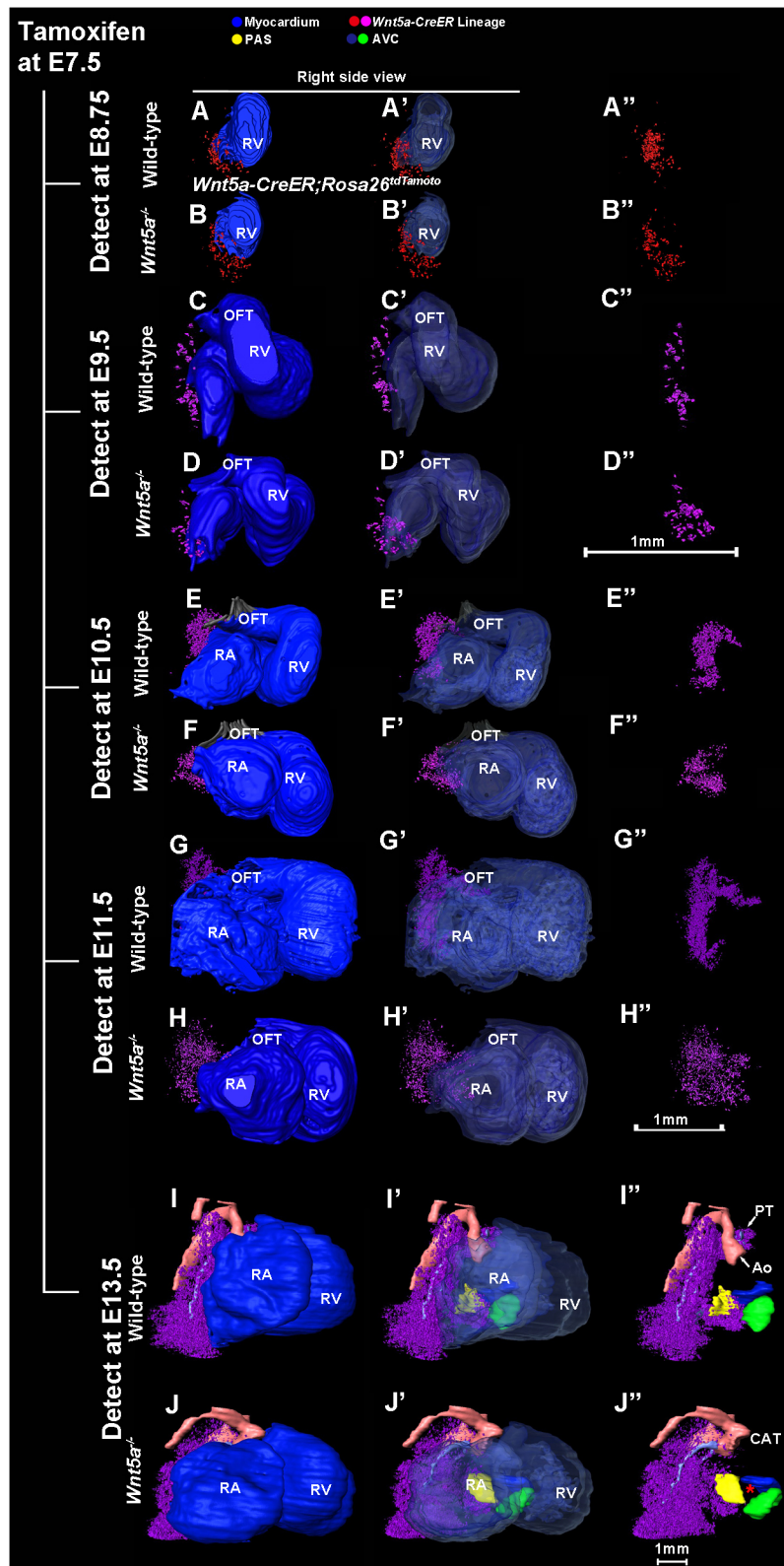


Fig. 4. The *Wnt5a* lineage in the SpM-SHF undergoes polarized and temporally distinct deployment to form the pulmonary trunk and DMP. (A-J'') To determine temporally how the *Wnt5a* lineage was deployed to the heart, *Wnt5a*-CreER; *Rosa26*^{tdTomato} embryos were treated with a single dose of tamoxifen at E7.5 and analyzed at E8.75, E9.5, E10.5, E11.5 and E13.5. In wild type, *Wnt5a*-expressing cells labeled at E7.5 were clustered initially at the caudal SpM-SHF near the atria at E8.75 (A-A''). Some of them moved anteriorly, reaching the OFT by E9.5, entering the inferior OFT at E10.5 and E11.5 (C-C'', E-E'', G-G''), and eventually form the pulmonary trunk at E13.5 (I-I''). Some of them also extended caudally into the atria to form the DMP at E13.5 (G'', I''). In *Wnt5a*^{-/-} embryos, the labeled cells were located properly in the caudal SpM-SHF at E8.75 (B-B''), but displayed no anterior deployment (D-D'', F-F'') and could not enter the OFT by E11.5 (H-H'') or contribute significantly to the common arterial trunk (CAT) at E13.5 (J-J''). The caudal extension of these cells was also delayed at E11.5 (H''). They managed to form a shortened DMP by E13.5 (J''), but failed to fully septate the atria.

2012). By inducing this radial intercalation-like thinning process, *Wnt5a* helps to convert loosely packed SHF cells into an epithelial organization, thereby promoting SpM-SHF morphogenesis and deployment to the OFT. The accumulation of *Wnt5a* lineage in the caudal SpM (Fig. 4D'', F'', H'') and the overall thickening of the SpM-SHF (Fig. 10, P, Table 1) in *Wnt5a*^{-/-} mutants support this

model. The dramatic widening of the SpM-SHF in *Wnt5a*^{-/-} mutants (Fig. 1G, H), on the other hand, suggests that *Wnt5a* may regulate additional cellular behavior during SHF morphogenesis. To uncover other mechanisms that *Wnt5a* may use to restrict SpM-SHF widening, we examined actomyosin distribution in the plane of the SpM-SHF epithelium.

On ventral whole-mount views of E9.5 embryos stained with phalloidin, we found that the two lateral regions of the SpM-SHF (Fig. 5A,A'') display multicellular actin cables oriented along the A-P axis and towards the arterial pole of the heart. Immunostaining for ppMLC (diphosphorylated non-muscle myosin light chain 2) further revealed colocalization of active myosin complexes with the multicellular actin cables. These data are consistent with the previous report that SpM-SHF is under epithelial tension from the heart tube and the A-P oriented actomyosin cables are the cellular response to this tension (Cortes et al., 2018; Francou et al., 2017). On the other hand, we also found that the medial region of the posterior SpM-SHF (Fig. 5A,A'), directly above the atria, displays multicellular actomyosin cables oriented along the M-L axis and perpendicular to the A-P axis, reminiscent of those in extending fly germ band and elongating chick neural plate undergoing CE (Blankenship et al., 2006; Nishimura et al., 2012).

When we examined the SpM-SHF in *Wnt5a*^{-/-} mutants, we found that the A-P oriented actomyosin cables on the lateral sides are not disrupted (Fig. 5B,B''). In the medial region of the mutant SpM-SHF, however, we could no longer find multicellular actin cables. The ppMLC staining is also significantly reduced and no longer display an M-L bias (Fig. 5B,B'). Furthermore, the apical surface of cells appears to be reduced in the mutants (Fig. 5A',B'), and could be related to premature upregulation of cell adhesion following loss of Wnt5a (Lecuit and Lenne, 2007; Li et al., 2016). When we re-examined *Wnt5a* expression on serial transverse sections, we found that it is restricted to the medial and posterior half of the SpM-SHF where the M-L oriented actomyosin cables are normally observed (Fig. S4).

In fly germ band and chick neural plate, the M-L oriented actomyosin cables are known to exert directional contractility for planar polarized cell intercalation to restrict M-L widening and drive A-P elongation (Blankenship et al., 2006; Nishimura et al., 2012). Therefore, *Wnt5a* may provide similar mechanical force to narrow and elongate the SpM-SHF by regulating M-L oriented actomyosin cables and contractility.

Wnt5a functions through Daam1 to regulate SpM-SHF development

Our data so far are consistent with the idea that *Wnt5a* acts as a PCP ligand to regulate morphogenesis in the mouse (Qian et al., 2007; Sinha et al., 2012; Wang et al., 2011). A number of earlier studies, however, proposed that *Wnt5a* functions through other mechanisms such as antagonizing canonical Wnt (Cohen et al., 2012; Mikels and Nusse, 2006; Nemeth et al., 2007; Topol et al., 2003). To delineate the molecular cascade underlying *Wnt5a* during SHF development, we tested whether *Wnt5a* acts through Daam1, a Diaphanous family Formin homology (FH) protein identified as a PCP effector downstream of non-canonical Wnt and Dvl in *Xenopus* (Habas et al., 2001; Liu et al., 2008). Daam1 has potent actin-polymerizing and -bundling activities (Jaiswal et al., 2013), and the current model proposes that Daam1 exists in an auto-inhibited form due to intra-molecular bond between its N-terminal GBD (GTPase binding domain) and C-terminal DAD (diaphanous auto-regulatory domain) domains. PCP activation by non-canonical Wnt enables Dvl to bind to the DAD domain, thereby disrupting the auto-inhibitory bond and activating Daam1 (Liu et al., 2008; Sato et al., 2006). Δ DAD, a

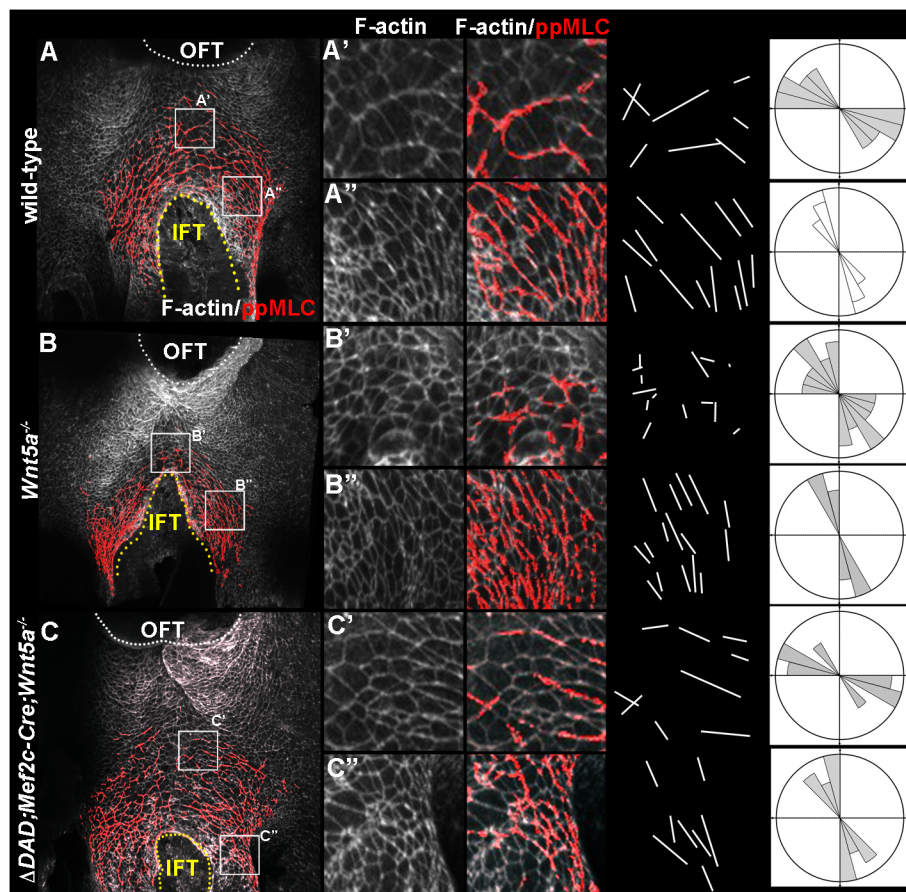


Fig. 5. Disruption of mediolaterally (M-L) oriented actomyosin distribution in *Wnt5a*^{-/-} mutant SpM-SHF. (A-C'') Ventral whole-mount views of E9.5 SpM-SHF stained with phalloidin and anti-ppMLC antibody (A-A'') reveal that the lateral region displays multicellular actin cables and ppMLC distribution oriented along the A-P axis (A''), while in the medial and posterior region they display M-L orientation (A'). (B-B'') In *Wnt5a*^{-/-} mutants, the A-P oriented actomyosin cables on the lateral sides are not disrupted (B''), but the ppMLC staining in the medial region is significantly reduced and with no M-L bias (B,B'). (C-C'') SHF-specific expression of Δ DAD restored M-L-oriented multicellular actomyosin cables in the medial SpM-SHF of the *Wnt5a*^{-/-} mutant (C') and rescue the SpM-SHF shortening defect (compare B with C). Schematic drawing of all discernable ppMLC cables in medial and lateral regions of each genotype was used to measure their angularity in relation to the A-P axis; their distribution is represented in rose diagrams in the right-most column.

Daam1 mutant lacking the DAD domain, is unable to form the auto-inhibitory bond and functions in a constitutively active fashion (Liu et al., 2008).

We therefore tested whether expressing Δ DAD in the SHF may rescue the cardiac defects in *Wnt5a*^{-/-} mutants. Using a BAC containing the genomic region of *Rosa26* locus, we created a conditional-activating *Rosa26- Δ DAD* BAC transgene by inserting Δ DAD behind a floxed 3xPoly(A) cassette that blocks transcription (Fig. 6A). We then used *Mef2c-Cre* to remove 3xPoly(A) and activate Δ DAD transcription in the SpM-SHF.

In *Wnt5a*^{-/-} mutants, *Rosa26- Δ DAD*; *Mef2c-Cre* can rescue both the DMP and OFT septation defect. Our 3D model showed that the atrial septation defect in *Wnt5a*^{-/-} mutants, caused by reduced DMP extension, is fully rescued in *Wnt5a*^{-/-}; *Rosa26- Δ DAD*; *Mef2c-Cre* embryos (Fig. 6G and J, *n*=8). Moreover, although *Wnt5a*^{-/-} mutants display a single unseptated OFT (Fig. 6E-G), expression of Δ DAD restored OFT septation, as evidenced by formation of two great arteries above the ventricles. However, rotation of the aorta and pulmonary trunk that normally occurs in the wild type is not rescued. All *Wnt5a*^{-/-}; *Rosa26- Δ DAD*; *Mef2c-Cre* hearts recovered

at E13.5 and later displayed DORV (*n*=8; Fig. 6H-J). Nevertheless, the ability of a constitutively active Daam1 to restore septation demonstrates that Wnt5a functions, at least in part, through the PCP effector Daam1 to regulate SHF development during OFT and atrial septation.

As our analyses of actin and ppMLC distribution suggested a link between Wnt5a function in regulating polarized SpM-SHF morphogenesis and M-L-oriented actomyosin cables (Fig. 5A-B"), we next investigated whether Δ DAD could also rescue diminished ppMLC in the medial SpM-SHF of *Wnt5a*^{-/-} mutants. Indeed, whole-mount staining of SpM-SHF from E9.5 *Wnt5a*^{-/-}; *Rosa26- Δ DAD*; *Mef2c-Cre* embryos revealed M-L-oriented ppMLC cables spanning several adjacent cells in the medial region, resembling those observed in the wild-type (Fig. 5C-C"). Associated with restoring M-L-oriented actomyosin cables in *Wnt5a*^{-/-} mutants, Δ DAD is also able to rescue the shortening of the SpM-SHF between the OFT and atria (compare the red lines in Fig. 6B,C and D; Fig. S5). These data support the hypothesis Wnt5a functions through Daam1 to exert the mechanical force for polarized SpM-SHF morphogenesis.

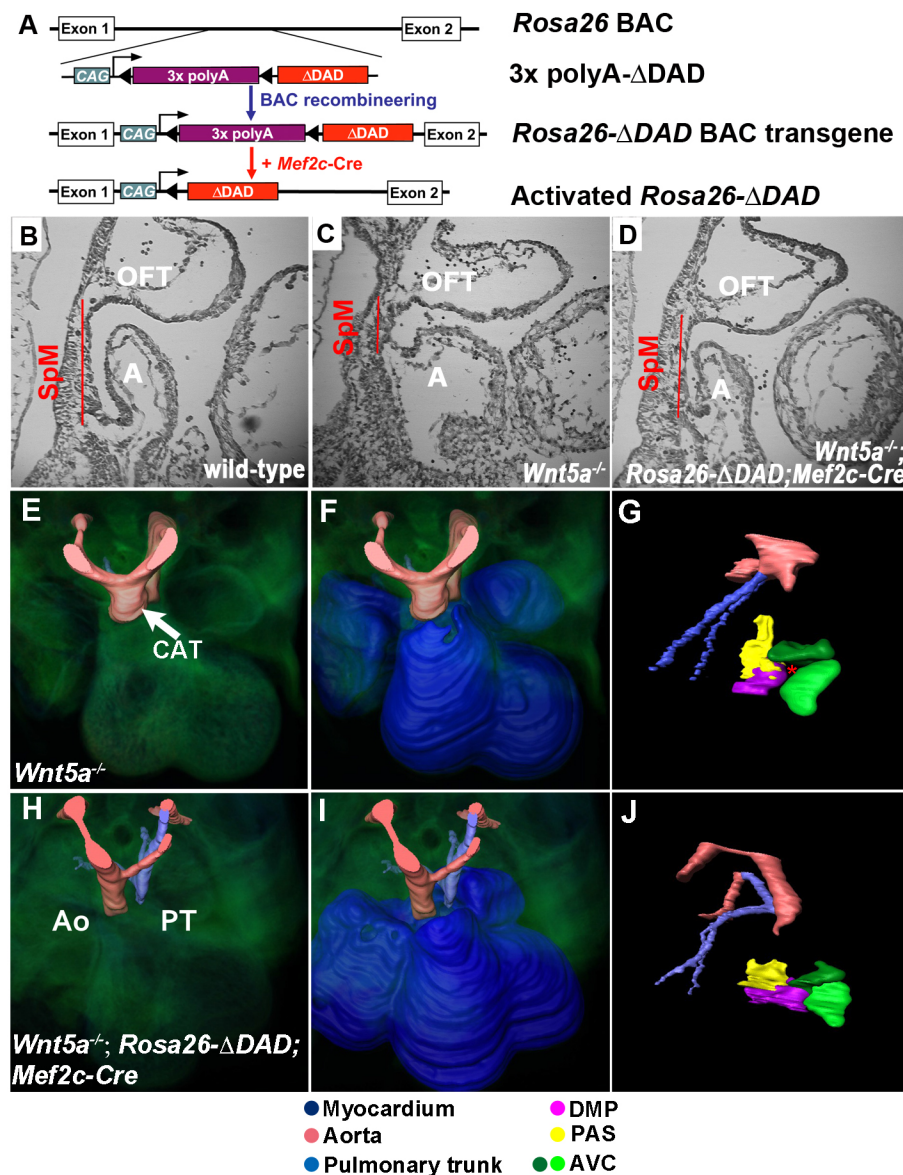


Fig. 6. Wnt5a functions through the PCP effector Daam1 to regulate SHF development. (A) The conditional *Rosa26- Δ DAD* was created by inserting a 3xpolyA- Δ DAD cassette into intron 1 of *Rosa26* in a BAC clone. (B-D) *Mef2c-Cre*-induced Δ DAD expression could rescue SpM-SHF shortening defect in *Wnt5a*^{-/-} mutant (compare red lines in C with D). (E-J) 3D reconstruction shows unseptated OFT (CAT, E,F) and shortened DMP unable to completely septate the atria (asterisk in G) in E13.5 *Wnt5a*^{-/-} mutant heart. *Mef2c-Cre*-induced Δ DAD expression fully rescued the atrial septation defect (J) and partially rescued the OFT defects by restoring OFT septation. (H,I) Proper rotation of the aorta and pulmonary trunk, however, is not rescued and *Wnt5a*^{-/-}; *Rosa26- Δ DAD*; *Mef2c-Cre* hearts display double outlet right ventricle.

DISCUSSION

The SHF harbors progenitor cells that are deployed and make a crucial contribution to the forming heart. In this manuscript, we used genetic labeling/tracing, 3D reconstruction and morphometric analyses, as well as genetic epistasis experiments to demonstrate that a *Wnt5a*→*Daam1* PCP signaling cascade regulates polarized morphogenesis of the SHF in the SpM (SpM-SHF). This morphogenesis may provide part of the morphogenetic force for SHF progenitor deployment towards both the arterial and venous poles for proper cardiac septation.

Polarized morphogenesis of the SpM-SHF

Previous studies have reported rapid proliferation of SHF progenitors in the SpM of avian embryos (van den Berg et al., 2009). Consistent with this finding, our genetic labeling with *Mef2c-Cre* showed that the volume of the SpM-SHF increases by approximately threefold from E10.0 to E11.5 (Table 1 and Fig. 1). With morphometric measurement, we further demonstrated that during this rapid growth period, the SpM-SHF did not expand isotropically. The increasing LWR and LTR in wild-type embryos indicate that the SpM-SHF length increases much more significantly than its width and thickness, providing the first evidence for a polarized morphogenesis process characteristic of CE in the SHF. In embryos lacking *Wnt5a*, a presumptive ligand that activates PCP signal to regulate CE, we found that the SpM-SHF became shorter, wider and thicker, although its overall volume remained similar to that in the wild type. More importantly, the LWR remains unchanged from E10.0 to E11.5 whereas the LTR is decreased in *Wnt5a* mutants, suggesting that, in the absence of *Wnt5a*, SpM-SHF growth becomes isotropic.

Wnt5a may play several roles to orchestrate polarized morphogenesis in the SpM-SHF. Based on histological and cell polarity studies, we previously proposed that *Wnt5a* might regulate cell cohesion and oriented cell intercalation at the caudal SpM to convert SHF cells from multi-layered mesenchyme into an epithelium (Li et al., 2016; Sinha et al., 2015a, 2012). Through this radial intercalation-like thinning process along the dorsoventral (D-V) axis, *Wnt5a* generates a morphogenetic force to lengthen the SpM and deploy SHF progenitors to the OFT, and possibly also to the DMP. The thickening of the SpM-SHF (Fig. 1) and the significantly reduced LTR in *Wnt5a* null mutant (Table 1) support our previous ideas. More direct evidence can also be found in the *Wnt5*-lineage tracing experiments, where descendants of pulse-labeled *Wnt5*-expressing cells, which are initially located at the caudal SpM at E8.75 (Fig. 4A"), normally extend anteriorly to the OFT from E9.5 to E11.5 (Fig. 4C",E",G"). In *Wnt5a* null mutants, *Wnt5a* lineage accumulated into a thickened mass at the caudal SpM and failed to extend anteriorly (Fig. 4D",F",H").

The above model, however, may not sufficiently explain normal SpM-SHF morphogenesis as D-V radial intercalation alone will result in even expansion of the surface area, and therefore proportionally increase both the length and width of the SpM-SHF. Instead, the increase of the width is much less than that of the length in wild type (Fig. 1). The significantly widened SpM-SHF (Fig. 1G,H) and the disruption of LWR increase in *Wnt5a* mutants (Table 1) implies that *Wnt5a* plays an additional role in restricting SpM-SHF widening. In both the mouse and chick, the most ventral layer of the SpM-SHF is organized into an atypical epithelium (Francou et al., 2017, 2014; Li et al., 2016; Sinha et al., 2015a, 2012; Soh et al., 2014; Waldo et al., 2005). In the medial region of the epithelial SpM-SHF, we found M-L-oriented multicellular actomyosin cables perpendicular to the A-P axis, along which the

SpM-SHF elongates (Fig. 5A,A"). These cables are enriched with activated forms of myosin light chains (di-phosphorylated at Thr18 and Ser19). They are most evident in the posterior and medial region of the SpM-SHF, where *Wnt5a* protein is specifically expressed (Fig. S4), and are disrupted in *Wnt5a* null mutants (Fig. 5B,B'). During neural tube closure in the chick, similar M-L-oriented actomyosin cables are controlled by PCP proteins, including *Celsr1*, *dishevelled* and *Daam1*. They exert planar-polarized contraction of adherens junctions for midline convergence, thereby driving A-P elongation and restricting M-L widening (Nishimura et al., 2012). We therefore propose that in the epithelial layer of the SpM-SHF, *Wnt5a*-induced PCP signaling may also promote M-L oriented contraction of the adherens junctions to drive SpM-SHF elongation and narrowing. The fact that SHF-specific expression of *ΔDAD*, an activated form of PCP effector *Daam1*, can restore M-L-oriented actomyosin cables and rescue A-P lengthening in *Wnt5a* null mutants is consistent with this idea (Fig. 5C,C'; Fig. 6C,D). Live imaging studies will be needed to test this idea in the future.

An elegant study by Francou et al. also carefully examined the epithelial layer of the SpM-SHF, and found that cells in the posterior SpM-SHF region display elongated apical surface and multicellular actomyosin cables towards the OFT, both of which are disrupted by blocking SHF deployment through transecting the OFT or mutation of *Tbx1* or *Nkx2.5* (Francou et al., 2017). These data led to the idea that the epithelial SpM-SHF is under tension associated with deployment of SpM-SHF to the OFT (Francou et al., 2017). We indeed also observed these OFT-oriented multicellular actomyosin cables, but only in the two lateral regions of the posterior SpM-SHF (Fig. 5A,A"). Interestingly, the OFT-oriented cell elongation and multicellular cables are not affected in *Wnt5a* null mutants (Fig. 5B, B'), despite severe disruption of SpM-SHF deployment, in contrast to *Tbx1* and *Nkx2.5* mutants (Francou et al., 2017). Therefore, it seems that OFT-oriented cell elongation and multicellular actomyosin cables may not be caused by SpM-SHF deployment per se but due to other sources, such as cardiac contraction (Francou et al., 2017) or a pulling force from the rostral SpM-SHF due to increased cell cohesion (Cortes et al., 2018; Francou et al., 2014; Li et al., 2016; Li and Wang, 2018). Irrespective of the source, the OFT-oriented mechanical signal may provide a key guidance cue, which functions together with *Wnt5a*/PCP to deploy SpM-SHF cell directionally towards the OFT (see below).

Wnt5a functions through the PCP pathway to regulate SpM-SHF development

The function of *Wnt5a* has been controversial in mammals. A number of studies, based in part on *in vitro* analyses, proposed that *Wnt5a* modulates canonical Wnt signaling through a variety of mechanisms (Baarsma et al., 2017; Bisson et al., 2015; Mikels and Nusse, 2006; Park et al., 2015; Topol et al., 2003). Other studies, in contrast, have primarily relied on phenotypic analyses of *Wnt5a* mouse mutants to address the role of endogenous *Wnt5a*, and found that loss of *Wnt5a* causes various morphogenesis defects, but not cell fate or proliferation defects common associated with canonical Wnt signaling. Furthermore, *Wnt5a* genetically interacts with core PCP gene such as *Vangl2* during limb, inner ear, OFT and neural tube development (Gros et al., 2010; Qian et al., 2007; Sinha et al., 2012; Wang et al., 2011). Therefore, endogenous *Wnt5a* appears to function primarily through PCP to regulate tissue shape and dimensions during embryonic development. The SpM-SHF morphogenesis defects we found in *Wnt5a* null and conditional mutants in the current study support this idea.

The apparent overlap between *Wnt5a* and *Wnt2/Wnt2b* expression in the caudal SpM-SHF nevertheless raises the possibility of cross-regulation between canonical and non-canonical Wnt pathways. By analyzing *Axin2* expression and cell proliferation, we previously found no evidence for perturbation of canonical Wnt activity in *Wnt5a* null or gain-of-function mutants (Li et al., 2016). In the current study, we further examined cell fate specification in the pulmonary mesoderm and found no defects in *Wnt5a* null mutants (data not shown), indicating that canonical Wnt-dependent pulmonary development is also unaffected. Conversely, our epistasis experiment showing partial rescue of SHF and OFT defects in *Wnt5* null mutants with Δ DAD, a constitutively active form of Daam1, provides more definitive genetic evidence that *Wnt5a* functions through the PCP pathway to regulate cardiac development.

The crucial role of endogenous *Daam1* in heart development has also been demonstrated by multiple cardiac defects in *Daam1* mutant mice, including DORV and ventricular noncompaction (Li et al., 2011). The ventricular noncompaction was attributed to a requirement of *Daam1* for actin cytoskeleton and sarcomeric organization in cardiomyocytes. The cause for DORV is less clear, although it is due to a requirement of *Daam1* in the *Nkx2.5-Cre*-positive lineage (Li et al., 2011). Given the expression pattern, both *Daam1* and its homolog *Daam2* are likely to function as PCP effectors in the SHF and the heart.

We note that Δ DAD is only able to partially rescue the cardiac defects in *Wnt5a* null mice, especially at the arterial pole. This could be due to expression level, timing or domain, or because Δ DAD is not able to fully recapitulate the function of PCP signaling. For example, proper PCP signaling may involve dynamic regulation of the on- and off-state of *Daam1*, or require additional effectors besides *Daam1*. In flies, *Daam1* is required for PCP during axon guidance but not epithelial polarization (Gombos et al., 2015). In the mouse, we found previously that expressing *Wnt5a* throughout the SHF leads to two deleterious effects: blocking addition of SHF cells to the OFT by reducing cell cohesion in the rostral SpM-SHF; and causing embryonic lethality by E13.5 for an unknown reason (Li et al., 2016). When we expressed Δ DAD throughout the SHF in the current study, we observed neither defect. Therefore, either Δ DAD expression in our current system is not high enough to mimic the effect of *Wnt5a* overexpression or *Wnt5a* has functions besides activating *Daam1*.

***Wnt5a-CreER* marks a unique SHF population that forms cardiac septation to enable pulmonary circulation**

Using transgenes and DiI injection as cell markers, we previously demonstrated a requirement for *Wnt5a* in deploying SpM-SHF cells to form the inferior OFT wall and its derivatives, including the subpulmonary myocardium (Sinha et al., 2015a). We reasoned that *Wnt5a* could act cell-autonomously or cell non-autonomously in the deployment process, and attempted to gain insight by mapping the fate of *Wnt5a*-expressing cells in wild-type and *Wnt5a* null mutants. Using the *Wnt5a-CreER* line, our lineage-tracing data showed that, in wild-type embryos, irrespective of the timing or dose of tamoxifen administration, *Wnt5a*-expressing SHF cells contribute to the distal inferior OFT wall and the DMP. Ultimately, they form the smooth muscle lining of the pulmonary trunk and the atrial septum at the arterial and venous poles, respectively (Figs 3 and 4).

Together with the lineage-tracing results in *Wnt5a* null mutants (Fig. 4), our data support the hypothesis that *Wnt5a* functions in an autocrine fashion because, in *Wnt5a* null mutants, *Wnt5a* lineage per se is stuck in the caudal SpM. Its arterial pole deployment fails almost completely (Fig. 4D''-J'') and its venous pole deployment is

delayed and reduced (Fig. 4H'', J''). On the other hand, the fact that the *Wnt5a* lineage does not contribute substantially to the proximal inferior OFT myocardium and its derivative, the subpulmonary myocardium, yet their formation is diminished in *Wnt5a* null mutants (Sinha et al., 2015a), implies that *Wnt5a* could also act cell-non-autonomously. This cell-non-autonomous action may be due to paracrine signaling to neighboring non-*Wnt5a*-expressing cells or to a pushing force generated by intercalating *Wnt5a*-expressing cells to displace non-*Wnt5a*-expressing cells towards the OFT and atria.

The *Wnt5a* lineage is very similar to the previously reported *Gli1* lineage (Hoffmann et al., 2009) in that they both contribute to the pulmonary trunk and DMP, suggesting that *Wnt5a* is expressed in Shh-responding cells in the SHF. Deleting *Shh* in pulmonary endoderm using *Nkx2.1-Cre* results in only atrial septal defects, whereas *Shh* deletion in the pharyngeal and pulmonary endoderm using *Nkx2.5-Cre* results in both OFT and atrial septal defects (Goddeeris et al., 2007; Hoffmann et al., 2009). These data led to the proposal that pharyngeal Shh signals to the aSHF for pulmonary trunk formation, whereas pulmonary Shh signals to pSHF for DMP formation (Hoffmann et al., 2009). Our temporal tracing of *Wnt5a-CreER* lineage, in contrast, indicates that a single cohort of cells in the pSHF contributes to both the pulmonary trunk and DMP formation (Fig. 4). Our data are consistent with the retrospective clonal analyses showing a close lineage relationship between the venous pole and the pulmonary trunk (Lescroart et al., 2012). A possible explanation for OFT septation defect being observed in the *Nkx2.5-Cre/Shh* but not in the *Nkx2.1-Cre/Shh* mutant is the timing of Cre expression. Indeed, our temporal tracing data indicate that, although *Wnt5a-CreER*-labeled caudal SpM-SHF cells contribute to both the OFT and DMP, their deployment to the OFT occurs ~2 days earlier than to the DMP (compare Fig. 4C'' with G''). Therefore, *Nkx2.1-Cre* may be expressed too late to delete *Shh* to impact OFT development.

What regulates the distinct timing and direction of pSHF deployment towards the OFT versus the DMP is an interesting question to be addressed in the future. Given that *Wnt5a*-mediated CE provides the morphogenetic force for deployment in both directions, we speculate that other cues may be needed for guidance. For example, the arterial pole-oriented mechanical tension described by Francou et al. (2017) may account for such a guidance cue that acts in parallel with *Wnt5a* for directional movement of pSHF cells towards the OFT. In this scenario, *Wnt5a* plays a permissive role, whereas other guidance cues play an instructive role, for SpM-SHF deployment.

Previous studies of a number of mouse lines with *Cre* insertion into genes including *Tbx1*, *Six2* and *Hoxb1* have reported that SHF cells contribute preferentially to the pulmonary trunk but much less to the aorta (Bertrand et al., 2011; Huynh et al., 2007; Zhou et al., 2017). The *Wnt5a-CreER* lineage displays the same bias, and is restricted primarily to the pulmonary trunk smooth muscle layer irrespective of the timing of tamoxifen induction. At the same time, the *Wnt5a-CreER* lineage also appears to be more restricted spatially at the venous pole than the other *Cre* lines, in that it contributes primarily to the DMP and much less to the atrial myocardial wall (Fig. 3). Temporally, genetic labeling with *Wnt5a-CreER* also contrasts that of *Six2-CreER*, which labels distinct heart structures depending on the time of tamoxifen injection (Zhou et al., 2017). Thus, the *Wnt5a* lineage appears to represent a unique subpopulation of pSHF progenitors that are specified very early during development (~E7.5-8.0), with a distinct role to form the atrial septum and the pulmonary trunk that enables separation of pulmonary from systemic circulation.

Lineage studies of the pSHF revealed that it contains multipotent ‘cardiopulmonary progenitors’, which contribute to both the venous pole of the heart and pulmonary mesoderm (Peng et al., 2013). A recent study further revealed that in the pSHF of amphibians and mice (but not in fish without lungs), expression of key cardiac transcription factor *Tbx5* initiates canonical Wnt signaling to specify the pulmonary endoderm, which in turn secretes Shh to promote pSHF cells for atrial septal formation (Steimle et al., 2018). These seminal findings have raised an important idea that an ancestral cardiac progenitor region could have been adopted for the coevolution of pulmonary and cardiac structures in tetrapods for terrestrial life. Interestingly, besides forming the atrial septum and pulmonary trunk to enable separate pulmonary circulation, *Wnt5a* lineage in the SpM-SHF also contributes extensively to the mesenchyme of the trachea, bronchi and lung (Fig. 3). Loss of *Wnt5a* causes severe trachea and lung morphogenetic defects (Kishimoto et al., 2018; Li et al., 2002) in addition to venous and arterial pole septation defects (Fig. 2 and Fig. S2), and we found that deleting *Wnt5a* with *Mef2cCre* is sufficient to cause upper airway defects such as shortening and widening of the trachea (Fig. S6). Therefore, our data suggest the intriguing possibility that, in parallel to the *Tbx5* transcription network for fate specification, *Wnt5a/PCP* is another molecular circuit recruited by the pSHF during the coevolution of heart and lung to coordinate morphogenesis of the pulmonary airways and the cardiac septations necessary for pulmonary circulation.

MATERIALS AND METHODS

Mouse strains and genotyping

Wnt5a null, *Wnt5a* conditional and *Wnt5a* gain-of-function *Rosa26^{Wnt5a}* mice were genotyped as reported previously (Cha et al., 2014; Ryu et al., 2013; Yamaguchi et al., 1999). *Mef2c-AHF-Cre*, *Islet1-Cre* and *Rosa26^{td-Tomato} Cre* reporter mice were maintained and genotyped as described previously (Madisen et al., 2010; Verzi et al., 2005; Yang et al., 2006).

To generate *Wnt5aCreER* BAC (bacterial artificial chromosome) transgenic mice, we acquired a 198 kb BAC clone RP23-357M9 that contains the mouse *Wnt5a* genomic region, from BACPAC Resource Center at Children’s Hospital Oakland Research Institute. Using BAC recombineering techniques, we inserted a tamoxifen-inducible CreER T2 cassette into *Wnt5a* genomic region to replace the entire exon 2, a strategy similar to that used to generate *Wnt11-CreER* BAC transgene (Sinha et al., 2015b). We acquired two independent *Wnt5aCreER* BAC transgenic lines and they display virtually identical labeling patterns when crossed to *Rosa26^{td-Tomato} Cre* reporter mice. *Wnt5a-CreER* BAC transgenic mice were genotyped by PCR using primers *CreA1* (CCG GGC TGC CAC GAC CAA) and *CreA2* (GGC GCG GCA ACA CCA TTT TT).

To generate *Rosa26-ΔDAD* BAC transgenic mice, we acquired a 206 kb BAC clone RP24-85L15 that contains the mouse *Rosa26* genomic region. We used BAC recombineering to insert *ΔDAD*, which encodes a constitutively active form of human DAAM1 mutant (Liu et al., 2008), into the intron 2 of *Rosa26*. A floxed cassette consisted of three tandem polyadenylation signals was placed in front of *ΔDAD* so that *ΔDAD* transcription can only be induced only upon Cre-mediated excision of the 3x *poly(A)* cassette. A *CAG* promoter was placed upstream of the floxed 3x *poly(A)* cassette to enhance transcription, and a woodchuck hepatitis virus posttranscriptional regulatory element (WPRE) was added downstream of *ΔDAD* to increase mRNA stability (Madisen et al., 2010). *Rosa26-ΔDAD* transgenic mice can be identified through PCR using primers F (GCA TCG ATC CGG AAC CCT TAA TAT AA) and R1 (TTG TAG ATG AAC TCG CCG) prior to *ΔDAD* activation. After *ΔDAD* activation, the transgene can be identified through PCR with primers F (GCA TCG ATC CGG AAC CCT TAA TAT AA) and R2 (CGG TGG TGC AGA TGA ACT TC). Animal care and use were in accordance with NIH guidelines and were approved by the Animal Care and Use Committee of the University of Alabama at Birmingham.

Embryo collection, sectioning and immunohistochemistry

Female mice were kept in a cage with a male and checked for vaginal plugs every day. The day when a plug was present was designated as E0.5. Embryos were dissected out at desired stages and fixed with 4% paraformaldehyde (PFA) overnight at 4°C. Fixed embryos or cardiac tissues were processed through a gradient of sucrose solutions and embedded in OCT, frozen with dry ice and kept at −80°C until use. Tissue blocks were sectioned on a cryostat (Leica CM3050) at 10 μm per section.

For immunohistochemistry, dried sections were washed with PBS and blocked with 10% normal goat serum in PBST for at least 1 h at room temperature before primary antibodies were applied. Primary antibodies used in this study were anti-cTnT (DSHB, RV-C2, 1:100), anti-SMA (Santa Cruz, SC-53015, 1:400), anti-ppMLC (Cell Signaling, 3674, 1:200) and anti-CD31 (BD, 550538, 1:400). Sections were incubated with primary antibodies overnight at 4°C before washing with PBST. Fluorophore-conjugated secondary antibodies and FITC-conjugated phalloidin (Sigma, P5282, 1:100) were then applied to sections for 2–3 h at room temperature. Stained sections were imaged under a laser scanning microscope (Olympus FV-1000) and subsequently analyzed with imaging software.

Tamoxifen administration for *Wnt5a-CreER* activation and genetic lineage tracing

Wnt5a-CreER mice were crossed with *Rosa26^{td-Tomato} Cre* reporter mice to obtain *Wnt5a-CreER*; *Rosa26^{td-Tomato}* embryos. Pregnant dams were administered tamoxifen (Sigma, T-5648; dissolved to 10 mg/ml in corn oil) at 2–4 mg/40 g body weight orally between 10am and 11am on the desired day(s). Embryos were fixed in 4% PFA at 4°C for 60 min to overnight depending on embryo stage, and subsequently stored in PBS. Bright-field and epi-fluorescent whole-mount embryo images were captured using a Leica MZ16FA fluorescence stereomicroscope equipped with a multi-fluorescent filter set and a DFC490 CCD camera.

Three-dimensional (3D) reconstruction

Serial cryo-sections from embryos or heart tissue were immunostained and imaged as previously described. Slices of images were then imported into 3D software Amira (V6.0, Thermo Scientific FEI) for reconstruction according to previous studies (Snarr et al., 2007b). Briefly, slices were first aligned using the sum of least square alignment algorithm. Additional manual alignment was performed to make appropriate adjustment using contours of phalloidin staining image. Segmentation was carried out on aligned slices using Td-tomato and cTnT staining as landmarks to generate volumes, which were subsequently smoothed using a 3D filter mask of three voxels for four or five iterations. At least three embryos or hearts were used for 3D reconstruction at each time point.

Whole-mount SpM staining and imaging

Whole-mount staining and imaging of SpM [also referred to as dorsal pericardial wall in by others (Francou et al., 2017)] was performed according to our previously published studies (Li et al., 2016; Sinha et al., 2015a). Briefly, embryo hearts, including the ventricles and atria, were removed to expose the SpM, leaving only the distal part of the OFT intact to serve as the landmark for the heart tube. SpM tissue was stained for ppMLC (Cell Signaling 3674) and phalloidin (Sigma P1951) as previously mentioned (Francou et al., 2017; Li et al., 2016; Sinha et al., 2015a). Whole SpM tissue after staining was mounted in silicon gel with ventral side facing up, and imaged with Olympus FV-1000 confocal microscope using a SUPER 20× immersion objective.

Acknowledgements

We thank Dr Raymond Habas for providing the *ΔDAD* construct and Dr Terry Yamaguchi for providing the *Wnt5a* gain-of-function *Rosa26^{Wnt5a}* mice. The anti-cTnT monoclonal antibody was obtained from the Developmental Studies Hybridoma Bank, created by the NICHD of the NIH and maintained at The University of Iowa, Department of Biology, Iowa City, IA 52242, USA.

Competing interests

The authors declare no competing or financial interests.

Author contributions

Conceptualization: D.L., J.W.; Methodology: D.L., A.A., J.W.; Formal analysis: D.L., J.W.; Investigation: D.L., A.A.; Resources: J.W.; Writing - original draft: D.L.; Writing - review & editing: J.W.; Visualization: D.L., A.A.; Supervision: J.W.; Project administration: J.W.; Funding acquisition: J.W.

Funding

This work was supported by grants from the National Institutes of Health (HL109130 and HL138470) to J.W. Deposited in PMC for release after 12 months.

Supplementary information

Supplementary information available online at
http://dev.biologists.org/lookup/doi/10.1242/dev.181719.supplemental

References

- Anderson, R. H., Chaudhry, B., Mohun, T. J., Bamforth, S. D., Hoyland, D., Phillips, H. M., Webb, S., Moorman, A. F. M., Brown, N. A. and Henderson, D. J. (2012). Normal and abnormal development of the intrapericardial arterial trunks in humans and mice. *Cardiovasc. Res.* **95**, 108-115. doi:10.1093/cvr/cvs147
- Baarsma, H. A., Skronska-Wasek, W., Mutze, K., Ciolek, F., Wagner, D. E., John-Schuster, G., Heinzmann, K., Günther, A., Bracke, K. R., Dagouassat, M. et al. (2017). Noncanonical WNT-5A signaling impairs endogenous lung repair in COPD. *J. Exp. Med.* **214**, 143-163. doi:10.1084/jem.20160675
- Bayly, R. and Axelrod, J. D. (2011). Pointing in the right direction: new developments in the field of planar cell polarity. *Nat. Rev. Genet.* **12**, 385-391. doi:10.1038/nrg2956
- Bertrand, N., Roux, M., Ryckebusch, L., Niederreither, K., Dollé, P., Moon, A., Capecchi, M. and Zaffran, S. (2011). Hox genes define distinct progenitor subdomains within the second heart field. *Dev. Biol.* **353**, 266-274. doi:10.1016/j.ydbio.2011.02.029
- Bisson, J. A., Mills, B., Paul Helt, J.-C., Zwaka, T. P. and Cohen, E. D. (2015). Wnt5a and Wnt11 inhibit the canonical Wnt pathway and promote cardiac progenitor development via the Caspase-dependent degradation of AKT. *Dev. Biol.* **398**, 80-96. doi:10.1016/j.ydbio.2014.11.015
- Blankenship, J. T., Backovic, S. T., Sanny, J. S. P., Weitz, O. and Zallen, J. A. (2006). Multicellular rosette formation links planar cell polarity to tissue morphogenesis. *Dev. Cell* **11**, 459-470. doi:10.1016/j.devcel.2006.09.007
- Boehm, B., Westerberg, H., Lesnicar-Pucko, G., Raja, S., Rautschka, M., Cotterell, J., Swoger, J. and Sharpe, J. (2010). The role of spatially controlled cell proliferation in limb bud morphogenesis. *PLoS Biol.* **8**, e1000420. doi:10.1371/journal.pbio.1000420
- Briggs, L. E., Kakarla, J. and Wessels, A. (2012). The pathogenesis of atrial and atrioventricular septal defects with special emphasis on the role of the dorsal mesenchymal protrusion. *Differentiation* **84**, 117-130. doi:10.1016/j.diff.2012.05.006
- Briggs, L. E., Phelps, A. L., Brown, E., Kakarla, J., Anderson, R. H., van den Hoff, M. J. and Wessels, A. (2013). Expression of the BMP receptor Alk3 in the second heart field is essential for development of the dorsal mesenchymal protrusion and atrioventricular septation. *Circ. Res.* **112**, 1420-1432. doi:10.1161/CIRCRESAHA.112.300821
- Bruneau, B. G. (2008). The developmental genetics of congenital heart disease. *Nature* **451**, 943-948. doi:10.1038/nature06801
- Butler, M. T. and Wallingford, J. B. (2017). Planar cell polarity in development and disease. *Nat. Rev. Mol. Cell Biol.* **18**, 375-388. doi:10.1038/nrm.2017.11
- Cha, J., Bartos, A., Park, C., Sun, X., Li, Y., Cha, S.-W., Ajima, R., Ho, H.-Y. H., Yamaguchi, T. P. and Dey, S. K. (2014). Appropriate crypt formation in the uterus for embryo homing and implantation requires Wnt5a-ROR signaling. *Cell Rep.* **8**, 382-392. doi:10.1016/j.celrep.2014.06.027
- Chang, C.-P. and Bruneau, B. G. (2012). Epigenetics and cardiovascular development. *Annu. Rev. Physiol.* **74**, 41-68. doi:10.1146/annurev-physiol-020911-153242
- Chen, L., Fulcoli, F. G., Ferrentino, R., Martucciello, S., Illingworth, E. A. and Baldini, A. (2012). Transcriptional control in cardiac progenitors: Tbx1 interacts with the BAF chromatin remodeling complex and regulates Wnt5a. *PLoS Genet.* **8**, e1002571. doi:10.1371/journal.pgen.1002571
- Cohen, E. D., Miller, M. F., Wang, Z., Moon, R. T. and Morrisey, E. E. (2012). Wnt5a and Wnt11 are essential for second heart field progenitor development. *Development* **139**, 1931-1940. doi:10.1242/dev.069377
- Cortes, C., Francou, A., De Bono, C. and Kelly, R. G. (2018). Epithelial properties of the second heart field. *Circ. Res.* **122**, 142-154. doi:10.1161/CIRCRESAHA.117.310838
- Devenport, D. (2016). Tissue morphodynamics: translating planar polarity cues into polarized cell behaviors. *Semin. Cell Dev. Biol.* **55**, 99-110. doi:10.1016/j.semdb.2016.03.012
- Etheridge, S. L., Ray, S., Li, S., Hamblet, N. S., Lijam, N., Tsang, M., Greer, J., Kardos, N., Wang, J., Sussman, D. J. et al. (2008). Murine dishevelled 3 functions in redundant pathways with dishevelled 1 and 2 in normal cardiac outflow tract, cochlea, and neural tube development. *PLoS Genet.* **4**, e1000259. doi:10.1371/journal.pgen.1000259
- Evans, S. M., Yelon, D., Conlon, F. L. and Kirby, M. L. (2010). Myocardial lineage development. *Circ. Res.* **107**, 1428-1444. doi:10.1161/CIRCRESAHA.110.227405
- Francou, A., Saint-Michel, E., Mesbah, K. and Kelly, R. G. (2014). TBX1 regulates epithelial polarity and dynamic basal filopodia in the second heart field. *Development* **141**, 4320-4331. doi:10.1242/dev.115022
- Francou, A., De Bono, C. and Kelly, R. G. (2017). Epithelial tension in the second heart field promotes mouse heart tube elongation. *Nat. Commun.* **8**, 14770. doi:10.1038/ncomms14770
- Goddeeris, M. M., Schwartz, R., Klingensmith, J. and Meyers, E. N. (2007). Independent requirements for Hedgehog signaling by both the anterior heart field and neural crest cells for outflow tract development. *Development* **134**, 1593-1604. doi:10.1242/dev.02824
- Goddeeris, M. M., Rho, S., Petiet, A., Davenport, C. L., Johnson, G. A., Meyers, E. N. and Klingensmith, J. (2008). Intracardiac septation requires hedgehog-dependent cellular contributions from outside the heart. *Development* **135**, 1887-1895. doi:10.1242/dev.016147
- Gombos, R., Migh, E., Antal, O., Mukherjee, A., Jenny, A. and Mihaly, J. (2015). The formin DAAM functions as molecular effector of the planar cell polarity pathway during axonal development in *Drosophila*. *J. Neurosci.* **35**, 10154-10167. doi:10.1523/JNEUROSCI.3708-14.2015
- Goodrich, L. V. and Strutt, D. (2011). Principles of planar polarity in animal development. *Development* **138**, 1877-1892. doi:10.1242/dev.054080
- Gros, J., Hu, J. K.-H., Vinegoni, C., Feruglio, P. F., Weissleder, R. and Tabin, C. J. (2010). WNT5A/JNK and FGF/MAPK pathways regulate the cellular events shaping the vertebrate limb bud. *Curr. Biol.* **20**, 1993-2002. doi:10.1016/j.cub.2010.09.063
- Habas, R., Kato, Y. and He, X. (2001). Wnt/Dishevelled activation of Rho regulates vertebrate gastrulation and requires a novel Formin homology protein Daam1. *Cell* **107**, 843-854. doi:10.1016/S0092-8674(01)00614-6
- Hoffmann, A. D., Peterson, M. A., Friedland-Little, J. M., Anderson, S. A. and Moskowitz, I. P. (2009). sonic hedgehog is required in pulmonary endoderm for atrial septation. *Development* **136**, 1761-1770. doi:10.1242/dev.034157
- Huebner, R. J. and Wallingford, J. B. (2018). Coming to consensus: a unifying model emerges for convergent extension. *Dev. Cell* **46**, 389-396. doi:10.1016/j.devcel.2018.08.003
- Humphries, A. C. and Mlodzik, M. (2018). From instruction to output: Wnt/PCP signaling in development and cancer. *Curr. Opin. Cell Biol.* **51**, 110-116. doi:10.1016/j.cub.2017.12.005
- Huynh, T., Chen, L., Terrell, P. and Baldini, A. (2007). A fate map of Tbx1 expressing cells reveals heterogeneity in the second cardiac field. *Genesis* **45**, 470-475. doi:10.1002/dvg.20317
- Jaiswal, R., Breitsprecher, D., Collins, A., Corrêa, I. R., Jr, Xu, M.-Q. and Goode, B. L. (2013). The formin Daam1 and fascin directly collaborate to promote filopodia formation. *Curr. Biol.* **23**, 1373-1379. doi:10.1016/j.cub.2013.06.013
- Kelly, R. G. (2012). The second heart field. *Curr. Top. Dev. Biol.* **100**, 33-65. doi:10.1016/B978-0-12-387786-4.00002-6
- Kishimoto, K., Tamura, M., Nishita, M., Minami, Y., Yamaoka, A., Abe, T., Shigeta, M. and Morimoto, M. (2018). Synchronized mesenchymal cell polarization and differentiation shape the formation of the murine trachea and esophagus. *Nat. Commun.* **9**, 2816. doi:10.1038/s41467-018-05189-2
- Lecuit, T. and Lenne, P.-F. (2007). Cell surface mechanics and the control of cell shape, tissue patterns and morphogenesis. *Nat. Rev. Mol. Cell Biol.* **8**, 633-644. doi:10.1038/nrm2222
- Lescroart, F., Mohun, T., Meilhac, S. M., Bennett, M. and Buckingham, M. (2012). Lineage tree for the venous pole of the heart: clonal analysis clarifies controversial genealogy based on genetic tracing. *Circ. Res.* **111**, 1313-1322. doi:10.1161/CIRCRESAHA.112.271064
- Li, D. and Wang, J. (2018). Planar cell polarity signaling in mammalian cardiac morphogenesis. *Pediatr. Cardiol.* **39**, 1052-1062. doi:10.1007/s00246-018-1860-5
- Li, C., Xiao, J., Hormi, K., Borok, Z. and Minoo, P. (2002). Wnt5a participates in distal lung morphogenesis. *Dev. Biol.* **248**, 68-81. doi:10.1006/dbio.2002.0729
- Li, D., Hallett, M. A., Zhu, W., Rubart, M., Liu, Y., Yang, Z., Chen, H., Haneline, L. S., Chan, R. J., Schwartz, R. J. et al. (2011). Dishevelled-associated activator of morphogenesis 1 (Daam1) is required for heart morphogenesis. *Development* **138**, 303-315. doi:10.1242/dev.055566
- Li, D., Sinha, T., Ajima, R., Seo, H.-S., Yamaguchi, T. P. and Wang, J. (2016). Spatial regulation of cell cohesion by Wnt5a during second heart field progenitor deployment. *Dev. Biol.* **412**, 18-31. doi:10.1016/j.ydbio.2016.02.017
- Liu, W., Sato, A., Khadka, D., Bharti, R., Diaz, H., Runnels, L. W. and Habas, R. (2008). Mechanism of activation of the Formin protein Daam1. *Proc. Natl. Acad. Sci. USA* **105**, 210-215. doi:10.1073/pnas.0707277105
- Madisen, L., Zwingman, T. A., Sunkin, S. M., Oh, S. W., Zariwala, H. A., Gu, H., Ng, L. L., Palmiter, R. D., Hawrylycz, M. J., Jones, A. R. et al. (2010). A robust and high-throughput Cre reporting and characterization system for the whole mouse brain. *Nat. Neurosci.* **13**, 133-140. doi:10.1038/nn.2467

- McCulley, D. J. and Black, B. L. (2012). Transcription factor pathways and congenital heart disease. *Curr. Top. Dev. Biol.* **100**, 253-277. doi:10.1016/B978-0-12-387786-4.00008-7
- Mikels, A. J. and Nusse, R. (2006). Purified Wnt5a protein activates or inhibits beta-catenin-TCF signaling depending on receptor context. *PLoS Biol.* **4**, e115. doi:10.1371/journal.pbio.0040115
- Nemeth, M. J., Topol, L., Anderson, S. M., Yang, Y. and Bodine, D. M. (2007). Wnt5a inhibits canonical Wnt signaling in hematopoietic stem cells and enhances repopulation. *Proc. Natl. Acad. Sci. USA* **104**, 15436-15441. doi:10.1073/pnas.0704747104
- Nishimura, T., Honda, H. and Takeichi, M. (2012). Planar cell polarity links axes of spatial dynamics in neural-tube closure. *Cell* **149**, 1084-1097. doi:10.1016/j.cell.2012.04.021
- Park, H. W., Kim, Y. C., Yu, B., Moroishi, T., Mo, J.-S., Plouffe, S. W., Meng, Z., Lin, K. C., Yu, F.-X., Alexander, C. M. et al. (2015). Alternative Wnt signaling activates YAP/TAZ. *Cell* **162**, 780-794. doi:10.1016/j.cell.2015.07.013
- Peng, T., Tian, Y., Boogerd, C. J., Lu, M. M., Kadzik, R. S., Stewart, K. M., Evans, S. M. and Morrisey, E. E. (2013). Coordination of heart and lung co-development by a multipotent cardiopulmonary progenitor. *Nature* **500**, 589-592. doi:10.1038/nature12358
- Person, A. D., Beiraghi, S., Sieben, C. M., Hermanson, S., Neumann, A. N., Robu, M. E., Schleiffarth, J. R., Billington, C. J., Jr, van Bokhoven, H., Hoogeboom, J. M. et al. (2010). WNT5A mutations in patients with autosomal dominant Robinow syndrome. *Dev. Dyn.* **239**, 327-337. doi:10.1002/dvdy.22156
- Qian, D., Jones, C., Rzadzinska, A., Mark, S., Zhang, X., Steel, K. P., Dai, X. and Chen, P. (2007). Wnt5a functions in planar cell polarity regulation in mice. *Dev. Biol.* **306**, 121-133. doi:10.1016/j.ydbio.2007.03.011
- Ramsbottom, S. A., Sharma, V., Rhee, H. J., Eley, L., Phillips, H. M., Rigby, H. F., Dean, C., Chaudhry, B. and Henderson, D. J. (2014). Vangl2-regulated polarisation of second heart field-derived cells is required for outflow tract lengthening during cardiac development. *PLoS Genet.* **10**, e1004871. doi:10.1371/journal.pgen.1004871
- Rana, M. S., Théveniau-Ruissy, M., De Bono, C., Mesbah, K., Francou, A., Rammah, M., Domínguez, J. N., Roux, M., Laforest, B., Anderson, R. H. et al. (2014). Tbx1 coordinates addition of posterior second heart field progenitor cells to the arterial and venous poles of the heart. *Circ. Res.* **115**, 790-799. doi:10.1161/CIRCRESAHA.115.305020
- Ryu, Y. K., Collins, S. E., Ho, H.-Y. H., Zhao, H. and Kuruvilla, R. (2013). An autocrine Wnt5a-Ror signaling loop mediates sympathetic target innervation. *Dev. Biol.* **377**, 79-89. doi:10.1016/j.ydbio.2013.02.013
- Sato, A., Khadka, D. K., Liu, W., Bharti, R., Runnels, L. W., Dawid, I. B. and Habas, R. (2006). Profilin is an effector for Daam1 in non-canonical Wnt signaling and is required for vertebrate gastrulation. *Development* **133**, 4219-4231. doi:10.1242/dev.02590
- Schleiffarth, J. R., Person, A. D., Martinsen, B. J., Sukovich, D. J., Neumann, A., Baker, C. V. H., Lohr, J. L., Cornfield, D. N., Ekker, S. C. and Petryk, A. (2007). Wnt5a is required for cardiac outflow tract septation in mice. *Pediatr. Res.* **61**, 386-391. doi:10.1203/pdr.0b013e3180323810
- Sinha, T., Wang, B., Evans, S., Wynshaw-Boris, A. and Wang, J. (2012). Disheveled mediated planar cell polarity signaling is required in the second heart field lineage for outflow tract morphogenesis. *Dev. Biol.* **370**, 135-144. doi:10.1016/j.ydbio.2012.07.023
- Sinha, T., Li, D., Théveniau-Ruissy, M., Hutson, M. R., Kelly, R. G. and Wang, J. (2015a). Loss of Wnt5a disrupts second heart field cell deployment and may contribute to OFT malformations in DiGeorge syndrome. *Hum. Mol. Genet.* **24**, 1704-1716. doi:10.1093/hmg/ddu584
- Sinha, T., Lin, L., Li, D., Davis, J., Evans, S., Wynshaw-Boris, A. and Wang, J. (2015b). Mapping the dynamic expression of Wnt11 and the lineage contribution of Wnt11-expressing cells during early mouse development. *Dev. Biol.* **398**, 177-192. doi:10.1016/j.ydbio.2014.11.005
- Snarr, B. S., O'Neal, J. L., Chintalapudi, M. R., Wirrig, E. E., Phelps, A. L., Kubalak, S. W. and Wessels, A. (2007a). Isl1 expression at the venous pole identifies a novel role for the second heart field in cardiac development. *Circ. Res.* **101**, 971-974. doi:10.1161/CIRCRESAHA.107.162206
- Snarr, B. S., Wirrig, E. E., Phelps, A. L., Trusk, T. C. and Wessels, A. (2007b). A spatiotemporal evaluation of the contribution of the dorsal mesenchymal protrusion to cardiac development. *Dev. Dyn.* **236**, 1287-1294. doi:10.1002/dvdy.21074
- Soh, B.-S., Buac, K., Xu, H., Li, E., Ng, S.-Y., Wu, H., Chmielowiec, J., Jiang, X., Bu, L., Li, R. A. et al. (2014). N-cadherin prevents the premature differentiation of anterior heart field progenitors in the pharyngeal mesodermal microenvironment. *Cell Res.* **24**, 1420-1432. doi:10.1038/cr.2014.142
- Steimle, J. D., Rankin, S. A., Slagle, C. E., Bekeny, J., Rydeen, A. B., Chan, S. S.-K., Kweon, J., Yang, X. H., Ikegami, K., Nadadur, R. D. et al. (2018). Evolutionarily conserved Tbx5-Wnt2/2b pathway orchestrates cardiopulmonary development. *Proc. Natl. Acad. Sci. USA* **115**, E10615-E10624. doi:10.1073/pnas.1811624115
- Topol, L., Jiang, X., Choi, H., Garrett-Beal, L., Carolan, P. J. and Yang, Y. (2003). Wnt-5a inhibits the canonical Wnt pathway by promoting GSK-3-independent beta-catenin degradation. *J. Cell Biol.* **162**, 899-908. doi:10.1083/jcb.200303158
- van den Berg, G., Abu-Issa, R., de Boer, B. A., Hutson, M. R., de Boer, P. A. J., Soufan, A. T., Ruijter, J. M., Kirby, M. L., van den Hoff, M. J. B. and Moorman, A. F. M. (2009). A caudal proliferating growth center contributes to both poles of the forming heart tube. *Circ. Res.* **104**, 179-188. doi:10.1161/CIRCRESAHA.108.185843
- van Vliet, P. P., Lin, L., Boogerd, C. J., Martin, J. F., Andelfinger, G., Grossfeld, P. D. and Evans, S. M. (2017). Tissue specific requirements for WNT11 in developing outflow tract and dorsal mesenchymal protrusion. *Dev. Biol.* **429**, 249-259. doi:10.1016/j.ydbio.2017.06.021
- Verzi, M. P., McCulley, D. J., De Val, S., Dodou, E. and Black, B. L. (2005). The right ventricle, outflow tract, and ventricular septum comprise a restricted expression domain within the secondary/anterior heart field. *Dev. Biol.* **287**, 134-145. doi:10.1016/j.ydbio.2005.08.041
- Waldo, K. L., Hutson, M. R., Ward, C. C., Zdanowicz, M., Stadt, H. A., Kumiski, D., Abu-Issa, R. and Kirby, M. L. (2005). Secondary heart field contributes myocardium and smooth muscle to the arterial pole of the developing heart. *Dev. Biol.* **281**, 78-90. doi:10.1016/j.ydbio.2005.02.012
- Wang, B., Sinha, T., Jiao, K., Serra, R. and Wang, J. (2011). Disruption of PCP signaling causes limb morphogenesis and skeletal defects and may underlie Robinow syndrome and brachydactyly type B. *Hum. Mol. Genet.* **20**, 271-285. doi:10.1093/hmg/ddq462
- Xie, L., Hoffmann, A. D., Burnicka-Turek, O., Friedland-Little, J. M., Zhang, K. and Moskowitz, I. P. (2012). Tbx5-hedgehog molecular networks are essential in the second heart field for atrial septation. *Dev. Cell* **23**, 280-291. doi:10.1016/j.devcel.2012.06.006
- Yamaguchi, T. P., Bradley, A., McMahon, A. P. and Jones, S. (1999). A Wnt5a pathway underlies outgrowth of multiple structures in the vertebrate embryo. *Development* **126**, 1211-1223.
- Yang, L., Cai, C. L., Lin, L., Qyang, Y., Chung, C., Monteiro, R. M., Mummery, C. L., Fishman, G. I., Cogen, A. and Evans, S. (2006). Isl1Cre reveals a common Bmp pathway in heart and limb development. *Development* **133**, 1575-1585. doi:10.1242/dev.02322
- Zhou, Z., Wang, J., Guo, C., Chang, W., Zhuang, J., Zhu, P. and Li, X. (2017). Temporally distinct Six2-positive second heart field progenitors regulate mammalian heart development and disease. *Cell Rep.* **18**, 1019-1032. doi:10.1016/j.celrep.2017.01.002